Transition metals supported on mesoporous ZrO_2 for the catalytic control of indoor CO and PM emissions

Pradeep Doggali [a], S. Waghmare [a], S. Rayalu [a], Y. Teraoka [b], Nitin Labhsetwar [a],[*]

[a] Environmental Material Division, National Environmental Engineering Research Institute (CSIR-NEERI), Nehru Marg, Nagpur 440020, India
[b] Department of Energy and Material Sciences, Faculty of Engineering Sciences, Kyushu University, Kasuga, Fukuoka 816-8580, Japan

ABSTRACT

Mesoporous ZrO_2 support has been prepared by using a low cost natural biopolymer chitosan as template, and different transition metals from the first row (Fe, Co, Ni, Cu and Mn) were impregnated on the synthesized support. The synthesized catalysts have been characterized by XRD, BET-SA, SEM, TEM, O_2-TPD and TG analysis to study the material details as well as to understand the catalytic mechanism. The activity of these catalysts has been investigated for CO and PM oxidation. Incorporation of transition metals improved the activity for both CO and PM oxidation. It has been observed that Co–ZrO_2 is the most active catalyst for studied reactions while, Ni based catalysts show the lowest activity for both the reactions. The transition metal supported catalysts follow the activity sequence Co–ZrO_2 > Mn–ZrO_2 > Cu–ZrO_2 > Fe–ZrO_2 > Ni–ZrO_2. The effect of CO_2, SO_2 and H_2O on CO oxidation activity was also investigated, and despite partial deactivation, the catalysts show good CO oxidation activity. The characterization of the materials by O_2-TPD studies explains the better catalytic performance for the Co–ZrO_2, Mn–ZrO_2 and Cu–ZrO_2 catalysts, as compared to Fe–ZrO_2 and Ni–ZrO_2. Such mesoporous zirconia with reasonably good surface area and without ordered structure could be useful for both CO and PM oxidation reactions.

© 2011 Elsevier B.V. All rights reserved.

1. Introduction

Use of solid fuels such as wood, crop residues, animal dung and coal for domestic applications in rural areas of India and other developing countries is the largest source of indoor air pollution. Carbon monoxide (CO) and particulate matter (PM) are the major pollutants released from these solid fuels, and contribute significantly to the serious health and environmental impacts [1,2]. National Institute of Occupational Health (NIOH), Ahmedabad, India reported indoor air CO levels of 144; 156; and 94 ppm during cooking by cow-dung, wood and coal, respectively [2]. Albalek et al. measured PM emissions and reported that daily exposure for women during the nonwork season was 15120 and 6240 $\mu g\,h^{-1}\,m^{-3}$ for the indoor and outdoor cooking villages, respectively [3]. These concentrations are substantially higher as per the air quality guidelines of WHO and United States Environmental Protection Agency (USEPA). Furthermore, a recent report published in Nature emphasized the adverse effects of soot particles on the atmosphere. As per this report, cook stoves may contribute about 40% of the black-carbon pollution in China and about two-thirds of the total in places such as India, Pakistan and Bangladesh

[4]. Respiratory illness, cancer, tuberculosis, parental outcomes including low birth weight, and eye diseases are the morbidities associated with indoor air pollution through solid fuel combustion [5]. A possible option to control these emissions could be introduction of catalyst in cook stove for the post combustion control of gaseous emissions. Such catalytic materials require high thermal as well as chemical stability.

Zirconium dioxide (ZrO_2) is an oxide with high melting point and high resistance for corrosion resulting in its stability as a catalyst support for many reactions [6]. In a previous study, we reported the monitoring and measurements of temperature of the exhaust and stove walls, in a view to consider a catalytic approach for emissions control from the cook stoves in rural areas [7]. The temperature available at the cookstove is sufficient for the catalytic activity. In addition to this, the interaction with the rural households regarding the impact of harmful indoor pollutants on their health, impelled us to explore these catalysts based technological interventions. In general, the rural population is willing to accept catalytic options. However, a great deal of awareness and training will be required for the successful implementation. Zirconia (ZrO_2) has earned wide interest as a catalyst for complete oxidation of hydrocarbons, volatile organic compounds and other reactions for environmental and energy related applications [8–11]. It has been reported that the anionic vacancies even in small amounts leads to better oxygen mobility in ZrO_2 [12]. In a recent study, we have

investigated Al_2O_3, ZrO_2 and TiO_2 as support materials for Cu–Mn bimetallic catalysts for both CO and PM oxidation reactions. These results suggest that ZrO_2 shows excellent activity despite its very low surface area as compared to Al_2O_3 and TiO_2 [7]. Mattheev et al. reported the CO oxidation over Co–ZrO_2 catalyst and concluded that this catalyst composition can easily be synthesized by incipient wetness method and high CO oxidation activity can be achieved by Co_3O_4 phase on monoclinic ZrO_2 [13]. Zou et al. examined the CO oxidation activity on Cu supported Al_2O_3, ZrO_2 and Al_2O_3 + ZrO_2 supported catalysts. The authors reported the enhanced activity of Cu–ZrO_2 system among the studied supports [14]. However, the activity of these catalysts strongly depends on the synthesis procedures and evaluation conditions. As mentioned before, ZrO_2 supported transition metal (Co and Cu) catalysts are not the new compositions for CO oxidation, it is still very important to know the active catalyst among the ZrO_2 supported Co, Mn, Fe, Cu and Ni for CO oxidation in presence of co-existing gases such as CO_2, SO_2 and water, as well for that of PM/soot oxidation. These studies can help in identifying the potential catalysts for the targeted application. In another previous article from our group we examined the catalytic behavior of zirconia supported Ru–Co bimetallic catalysts for diesel soot oxidation and demonstrated that excellent catalytic activity and good thermal stability of Ru can be achieved with ZrO_2 as a support [15]. This study further strengthens the potential of ZrO_2 support for PM/soot oxidation. In this way, the aim of the present investigation is to examine the catalytic properties of ZrO_2 supported transition metals (Co, Mn, Fe, Cu and Ni) for CO and PM/soot oxidation as well as to study the impact of SO_2, CO_2 and H_2O on CO oxidation activity. To overcome the limitations of zirconia with low surface area and small pores, mesoporous zirconia without ordered structure has been prepared and used in the present study.

2. Experimental

2.1. Synthesis of ZrO_2 support and catalysts

To synthesize mesoporous ZrO_2, 9 g of chitosan was added to 300 ml of 5% acetic acid solution and stirred using a laboratory stirrer for an hour. 21.96 g of zirconyl nitrate was dissolved in 50 ml of water. The above solution was then added to chitosan solution and vigorous stirring was continued for 3 h. The zirconium–chitosan solution was then added dropwise into 300 ml of 50% ammonia solution under stirring, to obtain the gel macrospheres. These macrospheres were stabilized in ammonia solution for 1 h. Gel macrospheres were then filtered and washed thrice with deionized water. Macrospheres were subsequently dried at ambient temperature for 24 h and calcined at a ramping rate of 1 °C/min up to 500 °C. The support thus obtained was ground in to powder, and aqueous solutions of nitrate salts of different transition metals (Fe, Co, Ni, Cu and Mn) in 10 mol% concentrations were added to the support. The mixture of support and metal nitrate solutions were stirred in a beaker for 3 h at 60 °C. Transition metal soaked support was then kept in an oven at 110 °C for 5 h for drying. The dried mass thus obtained was ground, homogenized and calcined at 500 °C in a furnace for 5 h. The similar procedure was followed to synthesize transition metal impregnated catalysts using commercially available ZrO_2. These catalysts were designated as Co–C–ZrO_2 for Co impregnated commercial ZrO_2, Mn–C–ZrO_2 for Mn impregnated commercial ZrO_2, Cu–C–ZrO_2 for Cu impregnated commercial ZrO_2, Fe–C–ZrO_2 for Fe impregnated commercial ZrO_2, Ni–C–ZrO_2 for Ni impregnated commercial ZrO_2, respectively.

3. Characterization of materials and evaluation of catalytic activity

XRD patterns were recorded on a Rigaku Rint-220HF diffractometer, operated at 40 kV and 50 mA with a monochromator and using Cu Kα radiations (λ = 0.15418 nm). Indexing of XRD peaks was done, by using JCPDS database for the respective phases. Surface area was measured by nitrogen adsorption method using automatic gas adsorption apparatus BELSORP 28SA (produced by Nippon Bell Co.) and data were evaluated by BET method. The samples were pre-treated at 300 °C before the nitrogen adsorption experiments. Elemental analysis of the catalytic materials was carried out using Perkin-Elmer ICP-OES 4100 BV instrument to determine the copper and manganese contents in catalysts. The SEM investigations were carried out by using HITACHI S-5000 instrument with 20.0 kV acceleration voltage and 1000× and 8000× magnifications. The structural details of the materials were also studied by high resolution transmission electron microscopy (HR-TEM) using JEOL JEM 3010 microscope operated at 300 kV (LaB_6 cathode, point resolution 1.7 Å). Electron diffraction patterns were evaluated using the Process Diffraction software package. Sample was dispersed in ethanol and treated in ultrasound for 10 min. A drop of very dilute suspension was placed on a holey-carbon-coated copper grid and allowed to dry by evaporation at ambient temperature [16]. Temperature-programmed desorption (TPD) study also carried out using the same Thermo Quest TPD/R/O 1100 analyzer. Prior to each run, the catalyst was heated up to 500 °C under the helium flow (30 NmL/min). After 30 min of isothermal heating at this temperature, the temperature was lowered to 25 °C in air flow. Afterwards, helium was fed to the reactor at 10-mL/min-flow rate and kept flowing for 1 h at room temperature in order to purge out any excess oxygen. The catalyst was then heated up to 500 °C at the constant heating rate of 10 °C/min under the same helium flow and O_2 desorbed during the heating was determined to study the TPD pattern.

3.1. Evaluation of catalytic activity

Catalytic activity of all the synthesized catalysts was investigated for CO and PM oxidation. The steady state, fixed bed gas evaluation assembly equipped with a quartz reactor, precise mass flow controllers (Alborg, USA) and heating system was used to carry out the CO oxidation reaction. 100 mg of catalyst was loaded in a fixed bed quartz reactor. Catalysts were pre-treated in He flow at 200 °C for 1 h for cleaning of surface. The reactant gas feed containing 2000 ppm CO, 10% O_2 and He balance was used for CO oxidation, and catalytic activity was measured at two different space velocities by analyzing the CO at the exit gas stream. CO was analyzed by a Shimadzu gas chromatograph using molecular sieve 5A column and TCD detector. CO oxidation reaction was also carried out in presence of CO_2, SO_2 and H_2O in feed gas composition. The PM/soot oxidation was studied by thermo gravimetric analysis using Rigaku-TAS-200 instrument and using commercially available black carbon (Degussa S.A, Printex-U) as a substitute for soot. The catalyst: carbon black weight ratio used was 95:5 and, the experiments were performed with tight contact condition, in which, the mixture of catalyst and carbon was ground in a mortar–pestle for 5 min. The blank TG experiments were also performed with only catalyst samples to account for any weight loss due to water desorption etc. Similar evaluation protocols are usually followed internationally for better comparison of catalytic results. A schematic of the experimental set up is given in Fig. 1.

4. Results and discussion

Fig. 2 illustrates the XRD patterns for synthesized mesoporous ZrO_2. These infer the tetragonal phase of synthesized mesoporous ZrO_2 sample and also suggest that the crystallinity of zirconia remains unaltered after impregnation with different transition metals. The predominant crystalline chitosan peaks at 2θ values 8°, 20° and 29° were not observed, which indicate the elimination
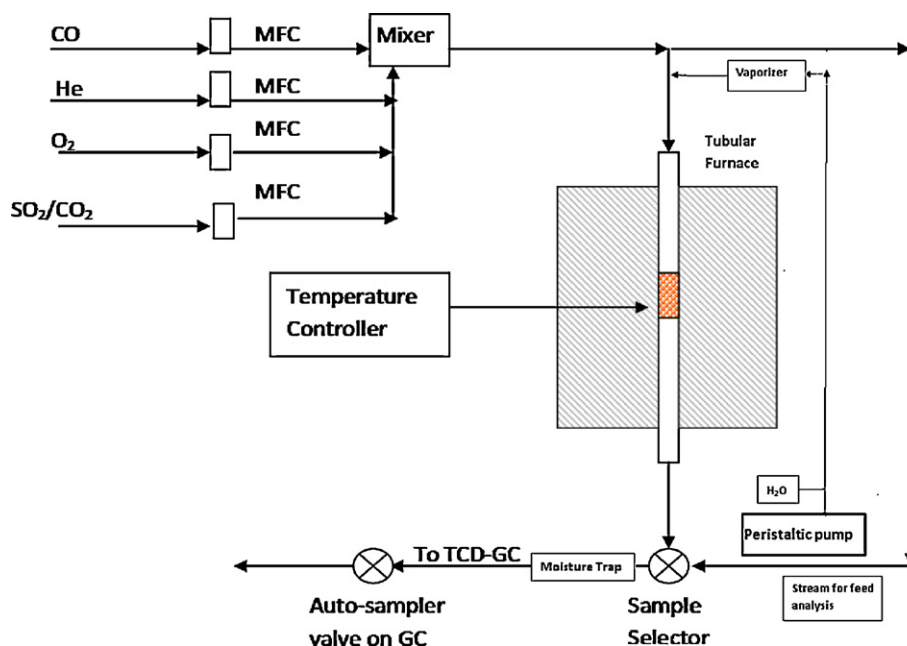
Fig. 1. Schematic of the experimental set up.
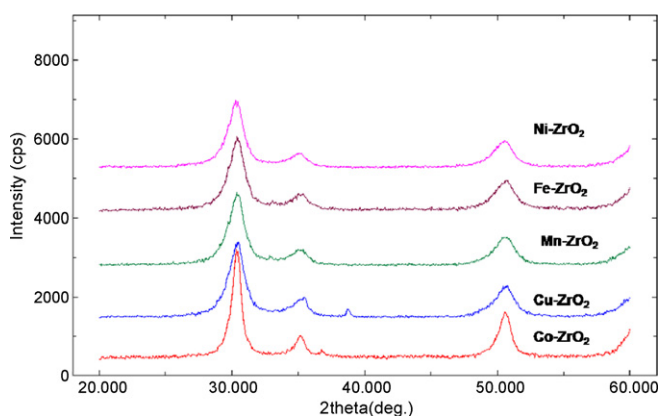
Fig. 2. XRD patterns of Co–ZrO$_2$, Mn–ZrO$_2$, Cu–ZrO$_2$, Fe–ZrO$_2$ and Ni–ZrO$_2$.

Table 1
Surface area and pore size results for Co–ZrO$_2$, Mn–ZrO$_2$, Fe–ZrO$_2$, Cu–ZrO$_2$ and Ni–ZrO$_2$.

S. no.	Sample	BET-surface area (m^2/g)	Pore diameter (nm)
1	Mesoporous ZrO$_2$	34.9	3.55
2	Co–ZrO$_2$	26.5	2.41
3	Mn–ZrO$_2$	25.2	2.34
4	Cu–ZrO$_2$	27.9	2.38
5	Fe–ZrO$_2$	26.8	2.33
6	Ni–ZrO$_2$	25.7	2.37

of template from the synthesized ZrO$_2$ [17]. No new peak in X-ray diffraction pattern was observed after incorporation of Mn, Fe and Ni on mesoporous ZrO$_2$ support, whereas Co–ZrO$_2$ and Cu–ZrO$_2$ show the characteristic peak of CuO and Co$_3$O$_4$, though the similar procedure was used to synthesize the catalysts. The N$_2$ BET surface area and pore characteristics results of the synthesized catalysts are presented in Table 1. These results clearly demonstrate that the synthesized ZrO$_2$ is mesoporous in nature and possess
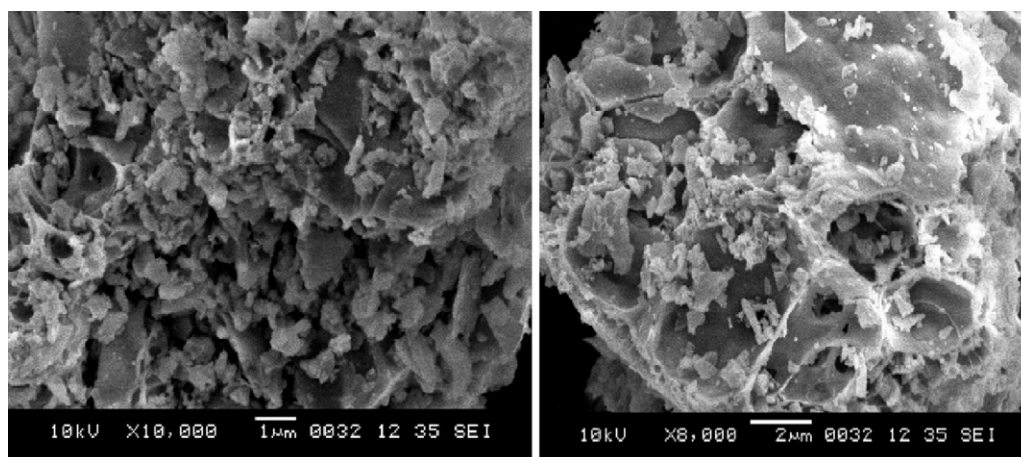
Fig. 3. SEM image of ZrO$_2$ synthesised by using the chitosan as template.
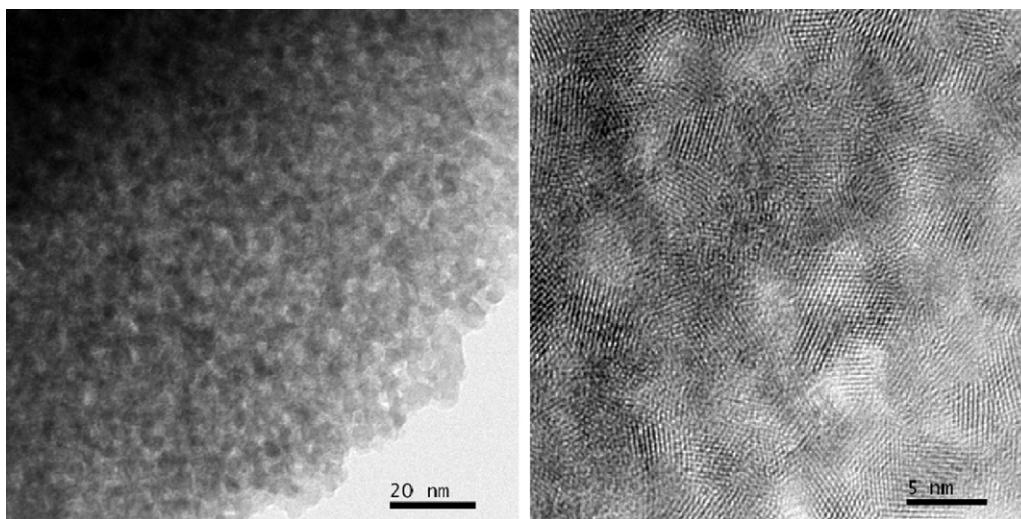
Fig. 4. TEM observations of ZrO_2 synthesised by using the chitosan as template.

reasonably high surface area without ordered structure. The results also indicate that surface area and pore size of the support have been slightly decreased after the impregnation of transition metals. This could be due to the formation of mixed oxide crystals on the pores of supports, thereby partially blocking the pore openings. The morphology and structure of the synthesized mesoporous zirconia was examined by scanning electron microscopy (SEM) and transmission electron microscopy (TEM). Fig. 3 represents the SEM images of the synthesized meso zirconia, which reveal presence of interconnected petal like structures on the surface of meso zirconia sample with sharp edges on the pore mouth. During calcination step of synthesis, volatile matter gets removed from the sample, leading to development of porous structures in the synthesized meso zirconia. TEM images (Fig. 4) display that mesoporous zirconia consists of sheets of aggregates of tetragonal ZrO_2 nanocrystals. Idiomorphic nanocrystals have well-developed crystal faces with size of about 50 nm. Electron diffraction pattern in Fig. 5, also confirm the tetragonal ZrO_2 structure (PDF 88-1007). Therefore, it can be inferred that it is possible to prepare mesoporous ZrO_2 without ordered structure using chitosan template.

4.1. CO oxidation activity

All the synthesized transition metal impregnated ZrO_2 catalysts were evaluated for their catalytic activity towards CO oxidation reaction. The CO oxidation activity as a function of temperature is shown in Fig. 6. From the results, it can be observed that, $Co–ZrO_2$ and $Mn–ZrO_2$ exhibit relatively high activity as compared to other investigated catalysts. These two catalysts get activated after about 80 °C and quickly achieve the light-off temperature, while $Cu–ZrO_2$ gets activated at 100 °C. On the other hand, the $Fe–ZrO_2$ and $Ni–ZrO_2$ start showing CO conversion at 160 °C and 180 °C respectively. The 100% CO conversion for $Co–ZrO_2$ and $Mn–ZrO_2$ was obtained at 140 °C and at approximately 30,000 h^{-1} space velocity, however T_i (temperature at which CO conversion started) and T_{50} (temperature at which 50% CO conversion observed) of the $Co–ZrO_2$ were observed to be lower than $Mn–ZrO_2$. The 100% CO conversion temperature for $Cu–ZrO_2$ is observed to be 180 °C, whereas this temperature was shifted to 220 °C for $Fe–ZrO_2$ and 280 °C for $Ni–ZrO_2$. The obtained results clearly indicate the higher catalytic activity of $Co–ZrO_2$ as compared to all the other catalysts studied.

4.1.1. Comparison of mesoporous ZrO_2 with the commercially available ZrO_2 support

The CO oxidation reaction was also performed with catalysts synthesized by using commercial ZrO_2 (HIMEDIA-Chemicals, S.A 16.7 m^2/g)) and following the same synthesis and evaluation conditions. Fig. 7 shows the CO oxidation activity results for the catalysts synthesized by using commercial ZrO_2. The 100% CO conversion temperature was shifted to 200 °C for $Co–ZrO_2$ thereby showing

Fig. 5. EDX pattern of ZrO_2 synthesised by using the chitosan as template. The green markers correspond to tetragonal ZrO_2.
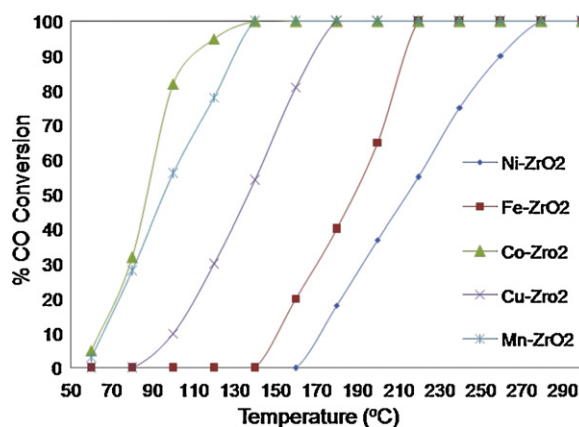
Fig. 6. CO oxidation over $Co–ZrO_2$, $Mn–ZrO_2$, $Cu–ZrO_2$, $Fe–ZrO_2$ and $Ni–ZrO_2$ Feed composition: CO = 2000 ppm, O_2 = 10% balance He at approximately 30,000 h^{-1} space velocity.

Table 2
Comparison of the CO oxidation activity for the catalysts synthesised with mesoporous supports and commercially available supports.

Catalysts	T_{10} °C	T_{50} °C	T_{90} °C	Rate (μ mol g^{-1} min^{-1} at 100 °C)	Rate (μ mol g^{-1} min^{-1} at 160 °C)
Co–ZrO$_2$	80	100	140	36.244	44.2
Mn–ZrO$_2$	80	100	140	24.75	44.2
Cu–ZrO$_2$	100	140	140	4.42	35.80
Fe–ZrO$_2$	160	200	180	0	4.42
Ni–ZrO$_2$	180	220	180	0	0
Co–C–ZrO$_2$	100	180	200	4.42	15.028
Mn–C–ZrO$_2$	140	180	220	0	12.37
Cu–C–ZrO$_2$	160	200	220	0	13.26
Fe–C–ZrO$_2$	200	240	260	0	0
Ni–C–ZrO$_2$	220	240	300	0	0

an increase of 60 °C. For Mn and Cu impregnated commercial ZrO$_2$ catalyst, the 100% CO conversion was observed at 220 °C, where as it was observed at 260 °C for Fe–ZrO$_2$ and 280 °C for Ni–ZrO$_2$. The shift in the temperature is mainly due to the lower surface area of the commercial zirconia support as compared to the present mesoporous support, synthesized by using the template method. The CO conversion rate for catalysts synthesized by using present mesoporous zirconia and commercial zirconia are given in Table 2. These results confirm that the T_{10}, T_{50} and T_{90} (temperature at which 90% CO conversion observed) temperatures for all the synthesized catalysts with mesoporous ZrO$_2$ are much lower than the catalysts prepared by using commercial ZrO$_2$ support.

4.1.2. Effect of space velocity on the catalytic activity for CO oxidation

Although space velocity of 30,000 h^{-1} is enough for the target application of present catalysts, we have studied the effect of higher space velocity on the catalytic activity. Fig. 8 shows the influence of space velocity on the CO oxidation activity for Co–ZrO$_2$, Mn–ZrO$_2$, Cu–ZrO$_2$, Fe–ZrO$_2$ and Ni–ZrO$_2$ catalysts. Catalytic activity in general was observed to slightly decrease with increase in space velocity (from 30,000 h^{-1} to 60,000 h^{-1}). The T_i for Co–ZrO$_2$ was shifted to 180 °C at 60,000 h^{-1}, where as the observed T_i for the Mn–ZrO$_2$ and Cu–ZrO$_2$ was 220 °C. The Fe–ZrO$_2$ shows 100% CO conversion at 260 °C, while Ni–ZrO$_2$ shows complete CO oxidation only after 300 °C. These results infer that although there is a slight shift in the T_i and T_f observed, the catalyst still show good CO oxidation activity at higher space velocities of 60,000 h^{-1}.

4.1.3. Impact of SO$_2$ on the catalytic activity for CO oxidation

When SO$_2$ (30 ppm) was introduced in the reaction stream, a decline in the catalytic activity was observed. This effect was however, more pronounced below 200 °C. Fig. 9 presents the impact of SO$_2$ (30 ppm) on the catalytic activity of Co–ZrO$_2$, Mn–ZrO$_2$, Cu–ZrO$_2$, Fe–ZrO$_2$ and Ni–ZrO$_2$. The 100% conversion temperature of Co–ZrO$_2$ and Mn–ZrO$_2$ has been shifted to 180 °C in presence of SO$_2$, where as it was observed to be 200 °C for Cu–ZrO$_2$ in presence of SO$_2$. The Fe–ZrO$_2$ and Ni–ZrO$_2$ show the 100% CO conversion only after 300 °C. The reported mechanism for SO$_2$ poisoning in presence of oxygen explains that SO$_2$ initially interacts with oxide surface
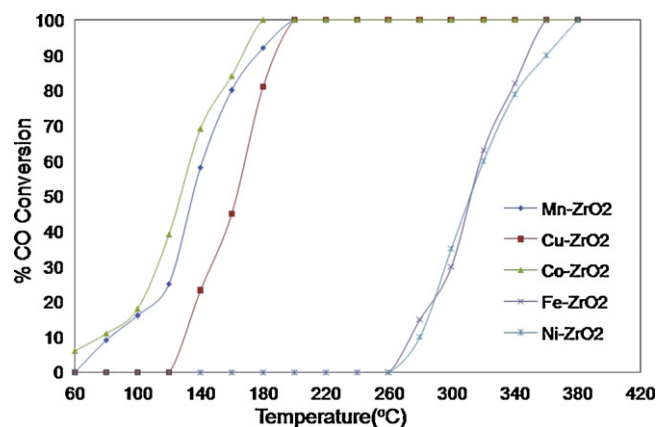
Fig. 8. Effect of space velocity on CO oxidation activity over Co–ZrO$_2$, Mn–ZrO$_2$, Cu–ZrO$_2$, Fe–ZrO$_2$ and Ni–ZrO$_2$. Feed composition: CO = 2000 ppm, O$_2$ = 10% balance He at approximately 60,000 h^{-1} space velocity.
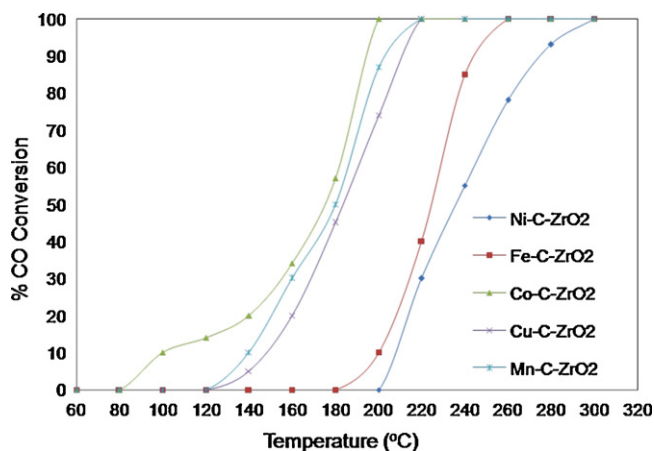
Fig. 7. CO oxidation over catalyst synthesised by using commercially available ZrO$_2$ (Co–C–ZrO$_2$, Mn–C–ZrO$_2$, Cu–C–ZrO$_2$, Fe–C–ZrO$_2$ and Ni–C–ZrO$_2$) Feed composition: CO = 2000 ppm, O$_2$ = 10% balance He at approximately 30,000 h^{-1} space-velocity.
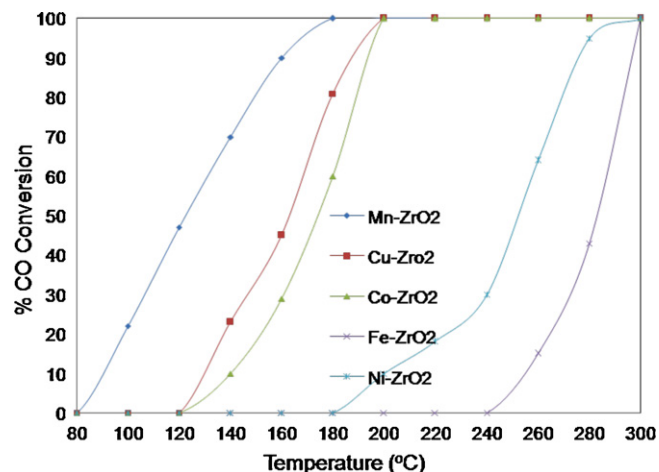
Fig. 9. Effect of SO$_2$ on the CO oxidation activity of Co–ZrO$_2$, Mn–ZrO$_2$, Cu–ZrO$_2$, Fe–ZrO$_2$ and Ni–ZrO$_2$, Feed composition: CO = 2000 ppm, O$_2$ = 10%, CO$_2$ = 3% balance He at approximately 30,000 h^{-1} space velocity.
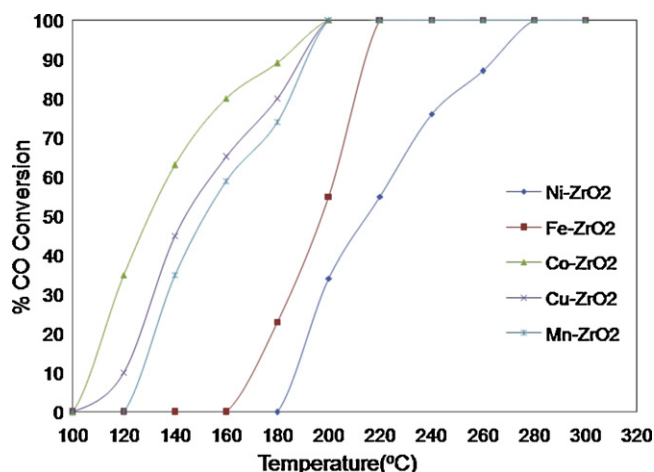
Fig. 10. Effect of H_2O on the CO oxidation activity of $Co–ZrO_2$, $Mn–ZrO_2$, $Cu–ZrO_2$, $Fe–ZrO_2$ and $Ni–ZrO_2$. Feed composition: CO = 2000 ppm, O_2 = 10%, H_2O (approximately 4 vol% balance) He at approximately 30,000 h^{-1} space velocity.

and forms reactive species such as SO_2^- after adsorption and are considered to react with surface oxygen of catalyst to form SO_3^- radicals. These formed species react with oxygen and are desorbed in the form of SO_4^- at high temperatures [18].

4.1.4. Effect of CO_2 on the catalytic activity for CO oxidation

When CO_2 (3 vol%), was introduced in the feed, no significant change in the catalytic activity was observed. This infers that the present catalysts are inert towards CO_2, which is always present in the solid fuel combustion exhaust. The observed activity order in presence of CO_2 was $Co–ZrO_2 > Mn–ZrO_2 > Cu–ZrO_2 > Fe–ZrO_2 > Ni–ZrO_2$, which is similar as observed in absence of CO_2.

4.1.5. Effect of H_2O on the catalytic activity for CO oxidation

In order to investigate the effect of water on the catalytic activity, experiments were performed by introducing approximately 4 vol% water in the feed gas composition (Fig. 10). A moderate decrease in the catalytic activity was observed for all the studied catalysts, however, the impact was significant only at lower temperatures. This slight shift in catalytic activity temperature indicates that the present catalyst compositions do not show severe impact of H_2O even at moderately high temperatures, which is almost always present with CO containing off gases from solid fuel combustion.

4.1.6. Mechanistic aspects

Intensive research has been subjected to study the mechanism of catalytic oxidation of CO in the past few decades and several mechanism have been proposed, mainly based on catalyst composition and the promoter elements used, as well as the reaction conditions. The CO oxidation over mixed oxide catalysts usually involves carbonate ion formation [19]. Based on DRIFTS studies, Luo et al. have also demonstrated the CO oxidation over mixed oxides type catalysts [20]. This mechanism can be applied to several mixed oxide type catalysts. As per this mechanism, the CO adsorbs on the catalyst surface and forms bidentate carbonate ion. The formed bidentate carbonate ion extracts surface lattice oxygen and creates oxygen vacancy. The adsorbed oxygen species, which is believed to be present possibly as O_2^- ion radicals, may react readily with the neighboring CO molecule adsorbed as bidentate carbonate, forming CO_2 again and recovering the catalyst surface. Considering the composition of present catalysts, we presume that the same mechanism could explain CO oxidation on present catalysts.

Table 3
TG results of Bare carbon, $Co–ZrO_2$, $Mn–ZrO_2$, $Fe–ZrO_2$, $Cu–ZrO_2$ and $Ni–ZrO_2$.

S. no.	Samples	T_i (°C)	$T_{50\%}$ (°C)	T_f (°C)
1	Bare Carbon	490	603	633
2	Co-ZrO2	330	485	592
3	Mn-ZrO2	374	490	594
4	Cu-ZrO2	391	519	583
5	Fe-ZrO2	444	558	619
6	Ni-ZrO2	485	566	617
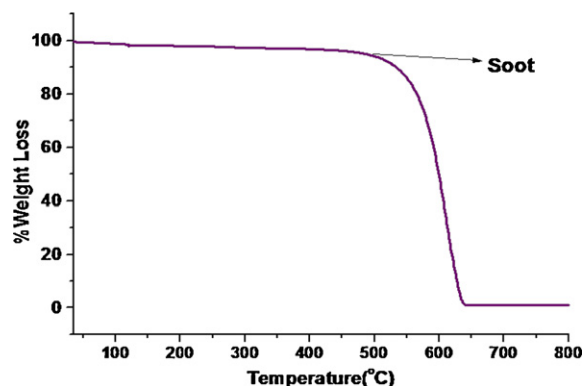
Fig. 11. Thermo gravimetric analysis (TG) results for catalytic soot oxidation.

4.2. Catalytic activity for PM/soot oxidation

The non catalytic combustion of PM/soot depends on many parameters such as amount of adsorbed hydrocarbons and experimental conditions, but generally exceeds 550 °C. In addition, the PM emissions released from soild fuel based cook stoves depend on quite a few parameters such as type of solid fuel used, moisture content, type of stove etc. Since it is difficult to collect PM with constant properties, commercially available model soot/carbon black Degussa S.A. (Printex-U) has been used with the following physical and chemical properties: fraction of adsorbed hydrocarbons (5.2%), ash (<0.1%), C (92.2%), H (0.6%), N (0.2%) and S (0.4%). The PM/soot oxidation was performed by thermo gravimetric analysis using Rigaku-TAS-200 equipment, wherein the mixture of soot and catalysts were heated at 5 °C/min from 35 °C to 800 °C, in air atmosphere and under the tight contact conditions. Table 3 presents the soot oxidation results for $Co–ZrO_2$, $Mn–ZrO_2$, $Cu–ZrO_2$, $Fe–ZrO_2$ and $Ni–ZrO_2$ with temperature values T_i (start of the carbon combustion) T_{50} (50% combustion of carbon) and T_f (complete combustion of carbon). It has been derived from Table 3, that non-catalyzed
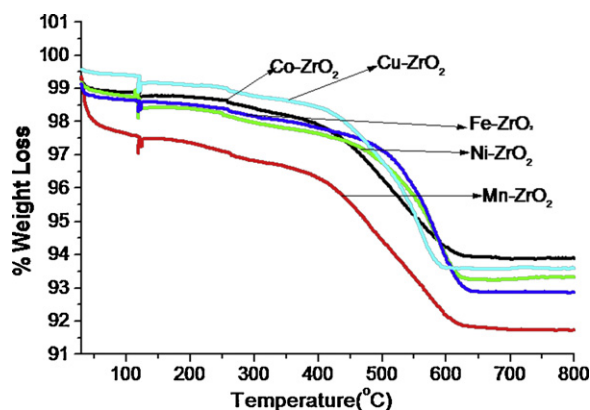
Fig. 12. Thermo gravimetric analysis (TG) results for $Co–ZrO_2$ + soot, $Mn–ZrO_2$ + soot, $Cu–ZrO_2$ + soot, $Fe–ZrO_2$ + soot and $Ni–ZrO_2$ + soot under tight contact condition.
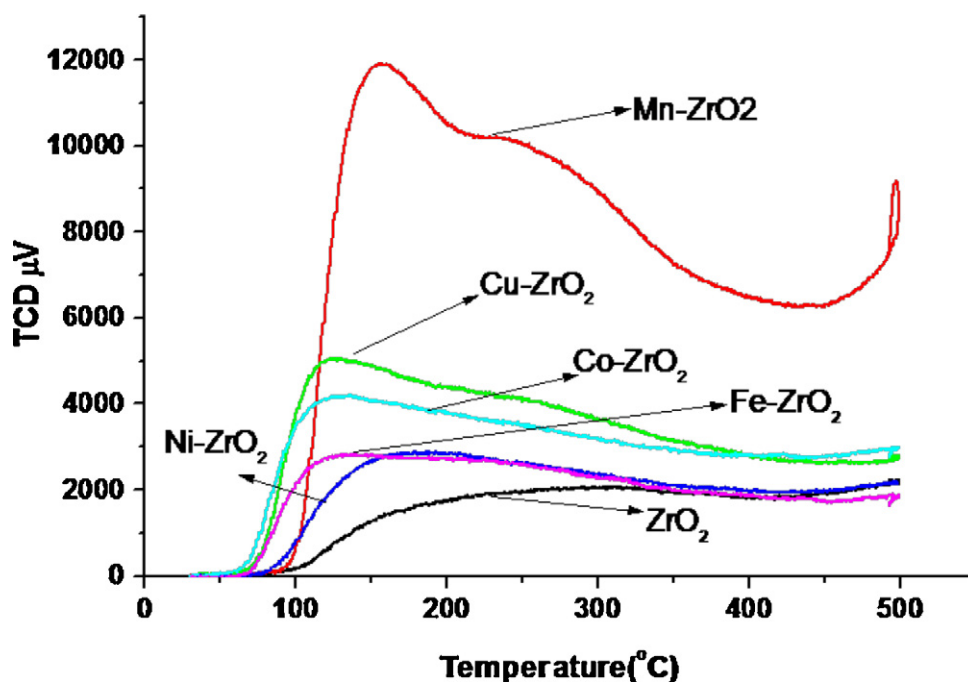
Fig. 13. O_2-TPD curves for ZrO_2, $Co–ZrO_2$, $Mn–ZrO_2$, $Cu–ZrO_2$, $Fe–ZrO_2$ and $Ni–ZrO_2$.

oxidation of carbon starts above 490 °C, while complete carbon oxidation was observed only after 633 °C, with a sharp weight loss due to carbon oxidation to CO_2. As it can be seen from Table 3, the T_i for the catalysts $Co–ZrO_2$, $Mn–ZrO_2$, $Cu–ZrO_2$, $Fe–ZrO_2$, and $Ni–ZrO_2$ are observed to be at 330 °C, 374 °C, 391 °C, 444 °C and 485 °C respectively, which are almost 150–200 °C lower than the non-catalyzed reaction. This can be considered as a good activity, though tight contact condition was used. Fig. 11 shows the non-catalytic oxidation of soot, while Fig. 12 shows the soot oxidation using $Co–ZrO_2$, $Mn–ZrO_2$, $Cu–ZrO_2$, $Fe–ZrO_2$, and $Ni–ZrO_2$ catalysts. These results clearly demonstrate the enhanced soot oxidation activity in presence of $Co–ZrO_2$, followed by $Mn–ZrO_2$, $Cu–ZrO_2$, $Fe–ZrO_2$, and $Ni–ZrO_2$. $Co–ZrO_2$ and $Mn–ZrO_2$ catalysts show T_i at 330 °C and 374 °C respectively, which is 160 °C and 116 °C lower than the non-catalyzed reaction. Though, T_i of the $Cu–ZrO_2$ is slightly higher than that of $Co–ZrO_2$ and $Mn–ZrO_2$, the T_f of the $Cu–ZrO_2$ is observed to be lower as compared to all the investigated catalysts. It is also apparent from Fig. 12, that $Fe–ZrO_2$ and $Ni–ZrO_2$ show T_i at 409 °C, 454 °C and T_f at 507 °C, 554 °C respectively. The observed values indicate the inferior activity of Fe and Ni supported ZrO_2 catalysts for soot oxidation reaction. J van Doorn et al. studied the soot oxidation reaction on the bare supports such as Al_2O_3, ZrO_2, V_2O_5, TiO_2, CeO_2 and La_2CO_3 [21]. Based on their results, the activity order was $V_2O_5 > CeO_2 > La_2CO_3$. TiO_2 and ZrO_2 show the similar activity, where as practically no soot oxidation activity was observed for Al_2O_3 and SiO_2. The present results support the above findings and infer that the redox properties of support also contribute towards catalytic soot oxidation. Various mechanisms have been proposed for soot oxidation reaction. From our previous studies on soot oxidation reaction on metal oxide and perovskites and their kinetic analysis, we presume that dissociative adsorption of oxygen could be the possible mechanism for soot oxidation activity [22–25].

For comparison, the PM oxidation activity was also evaluated for the catalysts synthesized by using the commercially available ZrO_2 ($Co–C–ZrO_2$, $Mn–C–ZrO_2$, $Fe–C–ZrO_2$, $Cu–C–ZrO_2$ and $Ni–C–ZrO_2$). However, no significant difference in the activity was observed. This suggests that the surface area may not be so significant for direct soot oxidation reaction.

4.3. O_2-TPD studies

Since the oxygen adsorption and desorption properties of the catalysts play important role for both CO and PM oxidation, O_2-TPD experiments were performed to understand the oxygen desorption on the investigated catalysts. Fig. 13 illustrates the O_2-TPD pattern for all the investigated catalysts (ZrO_2, $Co–ZrO_2$, $Cu–ZrO_2$, $Fe–ZrO_2$, $Mn–ZrO_2$ and $Ni–ZrO_2$). Two different types of oxygen species known as α and β were well defined in our previous O_2-TPD studies on mixed oxide materials for soot oxidation reaction [25]. The peaks at low temperatures are expected to be so called α oxygen species, which are weakly chemisorbed superficial oxygen species. Though, there is no considerable difference observed in the α oxygen desorption temperature of all the investigated catalysts, these catalysts show significant variation in the peak height corresponding to desorbed oxygen content. From TPD results, it is clear that the $Mn–ZrO_2$ appears to show high amount of α oxygen among the studied catalysts and the bare ZrO_2 shows the least. The amount of α oxygen released for the investigated catalysts follows the sequence $Mn–ZrO_2 > Cu–ZrO_2 > Co–ZrO_2 > Fe–ZrO_2 > Ni–ZrO_2$. The existence of alpha oxygen peaks in the temperature range of catalytic activity explained the better catalytic performances of these catalysts for both CO and PM oxidation reactions. $Mn–ZrO_2$ and $Cu–ZrO_2$ show large amount of α oxygen as compared to $Fe–ZrO_2$ and $Ni–ZrO_2$ catalysts, which could be considered as a direct evidence for the involvement of α-oxygen content towards catalytic oxidation activity of these oxide based catalysts. It has been observed in earlier studies, that the catalysts with higher amount of desorbed oxygen (α), indicate the higher amount of oxygen vacancies on catalyst surface. The formed oxygen vacancies can be correlated to the increase in oxidation activity. It is interesting to observe in the present study that, although $Co–ZrO_2$ does not show high amount of α oxygen, it shows the best catalytic activity for both CO and PM oxidation reactions. As mentioned earlier, several authors have studied the catalytic CO oxidation over Co based mixed oxide catalysts and reported that Co_3O_4 phase is very active for CO oxidation [26–29], which is also observed in the present catalyst. Presence of this phase could be the responsible reason for enhanced activity of $Co–ZrO_2$

for both CO and PM/soot oxidation reactions due to its redox properties. Therefore, the present O_2-TPD results demonstrate that, in addition to the oxygen vacancies formed in the catalyst, the active phase Co_3O_4 observed in case of Co–ZrO_2 also play a vital role and is responsible for the enhanced activity of Co–ZrO_2 catalyst for CO and PM/soot oxidation reactions.

5. Conclusion

Indoor air pollution caused by the soild fuel combustion in rural areas is recognized as one of the major environmental problems. Most of the work reported is related to the improvement in design of improved cook stoves or ventilation. Therefore, there exists a good potential for the catalytic applications. Our previous studies on emission monitoring data and temperature data collected from more than 100 rural households indicate that the exhaust temperature available is suitable for the application of catalyst. In the present work, mesoporous ZrO_2 support was synthesized by using chitosan as template and different transition metals form the first row (Co, Mn, Fe, Cu and Ni) have been supported using impregnation method. The catalytic activity of synthesized catalysts towards CO and PM oxidation has been investigated.

The XRD pattern of Co–ZrO_2 and Cu–ZrO_2 show the presence of crystalline transition metal oxide phases such as Co_3O_4 and CuO among all the synthesized catalysts, though the similar procedure was followed to synthesize these catalysts. The catalysts synthesized by using chitosan template show superior activity for CO oxidation than the catalyst synthesized by using commercial ZrO_2. This can be explained with the high surface area of the ZrO_2 synthesized by using template method. However, no significant difference in the catalytic activity for PM oxidation was observed with these catalysts as compared to the catalyst synthesized by using commercial zirconia. This suggests that the surface area is probably not so important for PM oxidation reaction. The Fe–ZrO_2 and Ni–ZrO_2 show the low amount of α oxygen in TPD among all the studied catalysts, which could be possible reason for the inferior activity of these catalysts. The Fe–ZrO_2 and Ni–ZrO_2 show the high temperature reduction peak and low amount of α oxygen in TPD among all the studied catalysts, which could be possible reason for the inferior activity of these catalysts. It is interesting to observe that, Co–ZrO_2 shows the enhanced activity as compared to all the investigated catalysts, though it does not show high amount of α oxygen as compared to Cu–ZrO_2 and Mn–ZrO_2. Thus the present O_2-TPD studies reveal that for the Co–ZrO_2 catalysts formation of oxygen vacancies are not so important and the active Co_3O_4 phase formed could be the possible reason for the enhanced activity of Co–ZrO_2 for both CO and PM/soot oxidation reactions.

The present mesoporous zirconia support with un-ordered structure shows excellent catalytic activity after metal incorporation, for the oxidation of CO even in presence of SO_2, CO_2, and water. Although, slight decrease in the catalytic activity was observed when SO_2 and water were introduced in the feed gas composition,

the effect appeared to be significant only at lower temperatures. We are working on development of catalyst coated structures as an innovative approach to possibly control the emissions from rural cook stoves, based on soild fuels.

Acknowledgements

References

[1] R.D. Edwards, Y. Liu, G. He, Z. Yin, J. Sinton, J. Peabody, K.R. Smith, Indoor Air 17 (2007) 189–203.
[2] S.T. Patel, C.V. Raiyani, in: P.R. Shukla (Ed.), Energy Strategies and Green House Gas Mitigation, Allied Publishers, New Delhi, 1995.
[3] R. Albalek, N. Bruice, J.P. Macracken, K.R. Smith, T.D. Gallardo, Environ. Sci. Technol. 33 (1999) 2505–2509.
[4] J. Tollefson, Nature 460 (2009) 29–32.
[5] N. Bruice, P. Padilla, R. Albalak, Bull. World Health Organ. 78 (2000) 1078.
[6] T. Yamaguchi, Catal. Today 20 (1994) 199–218.
[7] P. Doggali, H. Kusaba, H. Einaga, S. Bensaid, S. Rayalu, Y. Teraoka, Hazard. Mater. 186 (2010) 796–804.
[8] V.R. Choudhary, S. Banerjee, S.G. Pataskar, Appl. Catal. A 253 (2003) 65–74.
[9] J. Lamonier, M. Labaki, F. Wyrwalski, S. Siffert, A. Aboukais, J. Anal. Appl. Pyrolysis 81 (2008) 20–26.
[10] F. Wyrwalski, J.F. Lamonier, S. Siffert, A. Aboukais, Appl. Catal. B 70 (2007) 393–399.
[11] D. Dobber, D. Kiebling, W. Schmitz, G. Wendt, Appl. Catal. B 52 (2004) 135–143.
[12] C. Bozo, N. Guilhaume, J.-M. Herrmann, J. Catal. 203 (2001) 393–398.
[13] M. Yung, E. Holmgreen, U. Ozakan, Catal. Lett. 118 (2007) 180–186.
[14] R. Zhou, X. Jiang, J. Mao, X. Zheng, Appl. Catal. A 162 (1997) 213–222.
[15] M. Dhakad, D. Fino, S.S. Rayalu, R. Kumar, A. Watanabe, H. Haneda, S. Devotta, T. Mitsuhashi, N. Labhsetwar, Top. Catal. 42 (2007) 73–276.
[16] L.L. Janos, Ultramicroscopy 103 (2005) 237–249.
[17] D. Thakre, S. Jagtap, N. Sakhare, N. Labhsetwar, S. Meshram, S. Rayalu, Chem. Eng. J. 129 (2007) 173–180.
[18] R. Zhang, H. Alamdari, S. Kaliaguine, Appl. Catal. A: Gen. 340 (2008) 140–151.
[19] M.A. Pena, J.L. G.Fierro, Chem. Rev. 101 (2001) 1981–2017.
[20] Y. Luo, M. Meng, X. Li, X.G. Li, Y.Q. Zha, T.D. Hu, Y. Xie, J. Zang, J. Catal. 254 (2008) 310–324.
[21] J. Doorn, J. Varloud, P. Merraudeau, V. Perrrchon, Appl. Catal. B 1 (1992) 117–127.
[22] W.F. Shangguan, Y. Teraoka, S. Kagawa, Appl. Catal. B 12 (1997) 237–247.
[23] M. Dhakad, S. Rayalu, P. Doggali, S. Bakardjiva, J. Subrt, D. Fino, H. Haneda, N. Labhsetwar, Catal. Today 132 (2008) 188–193.
[24] N.K. Labhsetwar, M. Dhakad, S.S. Rayalu, R. Kumar, Top. Catal. 43 (2007) 299–302.
[25] M. Dhakad, N.K. Labhsetwar, S.S. Rayalu, R. Kumar, P. Doggali, Catal. Lett. 121 (2008) 137–143.
[26] P. Doggali, S. Kusaba, Y. Teraoka, P. Chankapure, S. Rayalu, N. Labhsetwar, Catal. Commun. 11 (2010) 665–669.
[27] J. Janson, A.E.C. Palmqvist, E. Fridell, M. Skoglundh, P. Osterlund, P. Thormahlen, Langer, J. Catal. 211 (2002) 387–403.
[28] J. Janson, J. Catal. 194 (2000) 55–59.
[29] S. Colonna, S. De Rossi, M. Faticanti, I. Pettiti, P. Porta, J. Mol. Catal. A 180 (2002) 161–168.